Original Study **Open Access**

Maciej Kożuch*, Łukasz Skrętkowicz

Proposal of concept for structural modelling of hybrid beams

https://doi.org/10.2478/sgem-2022-0023
received February 8, 2022; accepted August 30, 2022.

Abstract: Investigation on the behaviour of a *hybrid beam* is presented. Hybrid beam stands for an element with hybrid cross sections. This means sections that consist of steel and concrete parts, connected together with *composite dowels*, and both are considered for shear flow analysis. In practice, a more general solution may be used for bridges in the form of a beam in which the span sections are hybrid and the support sections are concrete. Recently such a solution has been introduced for bridge engineering in Poland and a new problem with performing a global analysis of hybrid beams was identified. The solution is new itself and requires also a new approach for internal forces determination. Discussion of this problem is made in the paper. Influences of (1) concrete cracking, (2) rheology of concrete and (3) methods of modelling on the redistribution of internal forces are highlighted. On an example of one of the real bridge girder (being currently under design) analysis is made to show how the abovementioned factors are affecting obtained results. Results are analysed and conclusions are presented. As a final step, a new concept of hybrid beam design is proposed. The proposed solution enables a quick and easy engineering approach to perform a static calculation of the considered structure.

Keywords: sand; mean grain size; mean pore size model; pore size distribution; water retention curve.

1 Introduction

The introduction in the last decade of new continuous open connectors, the so-called *composite dowels* [1-3], initiated the appearance on the market, mainly of bridge structures, of new structural forms. Typical composite structures where the steel part is an I-section (rolled or welded) and the concrete part is a deck slab can be replaced by beams where the steel part is made of T-sections (bottom flange + web) and the concrete part is a deck plate with web. In the cross section of such beams, the height of the steel web and its 'continuation' in the form of a concrete web can vary smoothly, resulting in free formability and effective optimisation (Fig. 1).

In 2016, the bridge structure shown in Figs 2–4 was built in Elbląg, Poland [4, 5]. The composite girder was designed with a variable cross section along the beam. In mid-spans, it consisted of a steel T-section with a high steel web connected to the concrete deck slab (see Fig. 1, section no. 2 and Fig. 4), and in regions of hogging bending moments (close to internal supports), the height of T-section's web was reduced, and instead, a concrete web with a variable increasing height toward the internal supports was introduced (see Fig. 1, section no. 4 and Fig. 4). This way, in mid-span regions, the self-weight of the girder was limited, and moreover, the steel part was applied in the tensile zone, while the concrete part was in

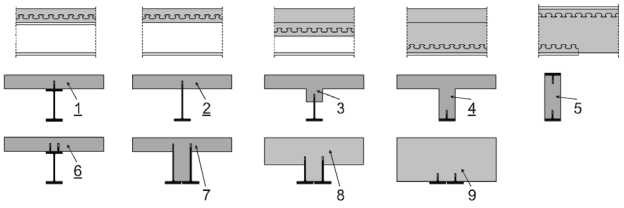

Figure 1: Different side views (upper row) and cross sections (middle and bottom rows) of girders with composite dowels. 1–5: With single dowel strip, 6–9: sections using two dowel strips [4].

Figure 2: Bridge in Elbląg using both steel and concrete webs in the girder [4, 5].

***Corresponding author: Maciej Kożuch,** Wrocław University of Technology, Wrocław, Poland, E-mail: maciej.kozuch@pwr.edu.pl
Łukasz Skrętkowicz, Wrocław University of Technology, Wrocław, Poland

the compressed zone. In a hogging moments region, the steel part remains to strengthen the narrow, compressed concrete part.

In 2018, another bridge was built [6] (Figs 5 and 6) in Sobieszewo, Poland, where the above solutions were developed. In the zone of hogging moments, the steel part was completely omitted, replacing the composite cross section with a reinforced concrete (RC) cross section. To do so, the so-called transition zone had to be introduced, thanks to which the steel element from the span part could be effectively anchored in the concrete part [7, 8]. This solution allowed for further optimisation of the structure, reducing the use of structural steel only to areas where it is necessary (in places where it would work as compressed, it was replaced with an RC section).

Many bridge structures located along the S3 road in Poland [9] are being designed currently, and a further evolution of hybrid beams is introduced in this design. This is because apart from the transition zone (slightly modified in comparison to the bridge in Sobieszewo), thin concrete webs (20 cm), which were thinner than the ones used so far, were introduced and going outside of ranges provided for composite dowels in the approvals [10-12]. To make it possible, a modification of the arrangement of reinforcing bars in the vicinity of the connectors was applied (the new name, strongly reinforced composite dowels [SRCD], was introduced), thus eliminating the destruction mechanism referred to as pry-out cone [1]. Europrojekt Gdańsk, in cooperation with the Wroclaw University of Technology, is responsible for the design of the bridges. Cross section of one of the bridges is presented in Fig. 7. For details of the beam, see also Fig. 12.

At the end of 2019, a railway bridge was built in Dąbrowa Górnicza [4, 13, 14], in which the U-shaped cross section of the structure consisted of two beam girders and an RC deck. Girder's webs are the side edges of the ballast truck (Figs 8 and 9). The main girders consist of steel T-sections placed both in the upper and lower zones of the girder, an RC web and the effective part of the RC deck. This bridge, designed by Fasys Mosty in collaboration with ArcelorMittal [14], appears to be a very economical solution for medium-span railway bridges.

Figure 3: Steel T-sections of Elbląg bridge. High T-sections for mid-span regions, low T-sections for internal support regions [4].

2 Problem identification

Design rules for objects such as the ones presented in Section 1 go beyond the framework described in the current design standards, for example, [15-17]. Apart from the composite dowels, the cross section of the girders has both steel and concrete parts, both of which are responsible for transferring the shear force. Taking into account the significant share of both the steel and concrete parts, it is not possible (or not economically justified) to design the cross sections assuming that the entire shear force is transmitted through the steel part (which is assumed in practice when designing a typical composite cross section

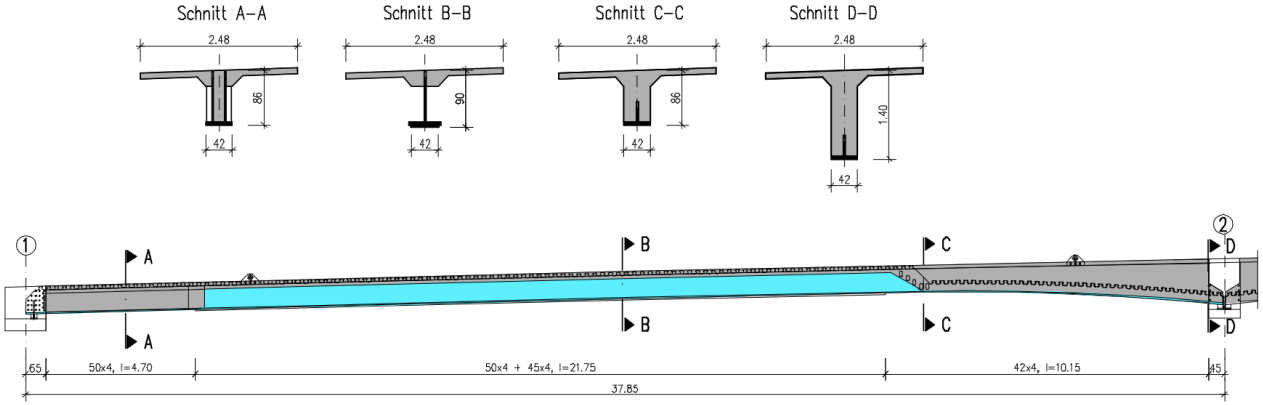

Figure 4: External span of the Elbląg bridge [4, 5].

Figure 5: Hybrid beams of Sobieszewo bridge [4, 6].

according to [17]). A new type of cross section, forcing the application of new design approaches due to the flow of shear stresses, is called hybrid section [4, 9, 18]. The issue of shear force transfer in such a cross section has already been described, and the dimensioning procedure is known at the level of cross section [18-21]. The cross section described in [20] as a general composite section is now called a hybrid section, and the name has been sanctioned internationally after discussions (Prof. Roger Johnson and Wojciech Lorenc) during work on the European technical approval for composite dowels [11]. While the concept of a

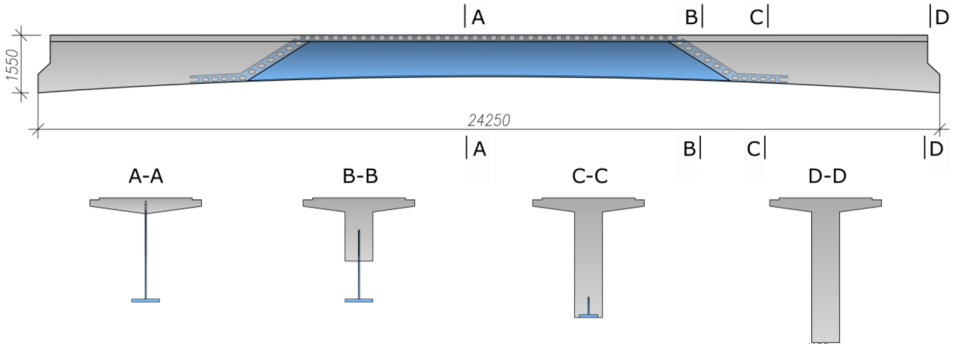

Figure 6: Hybrid girder of Sobieszewo bridge [7].

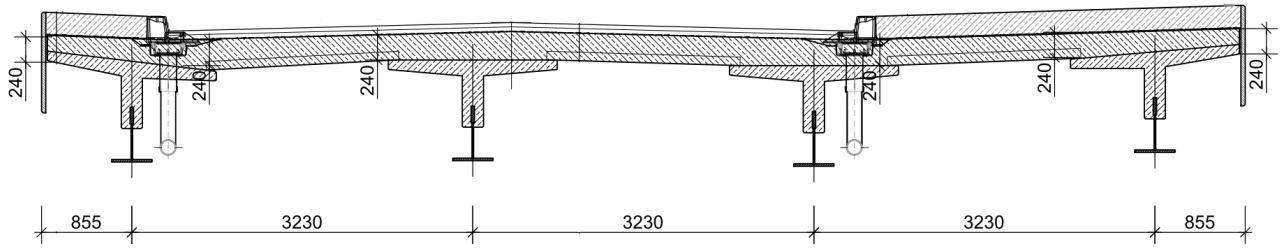

Figure 7: Cross section of one of the bridges along the S3 road being designed currently by Europrojekt Gdańsk.

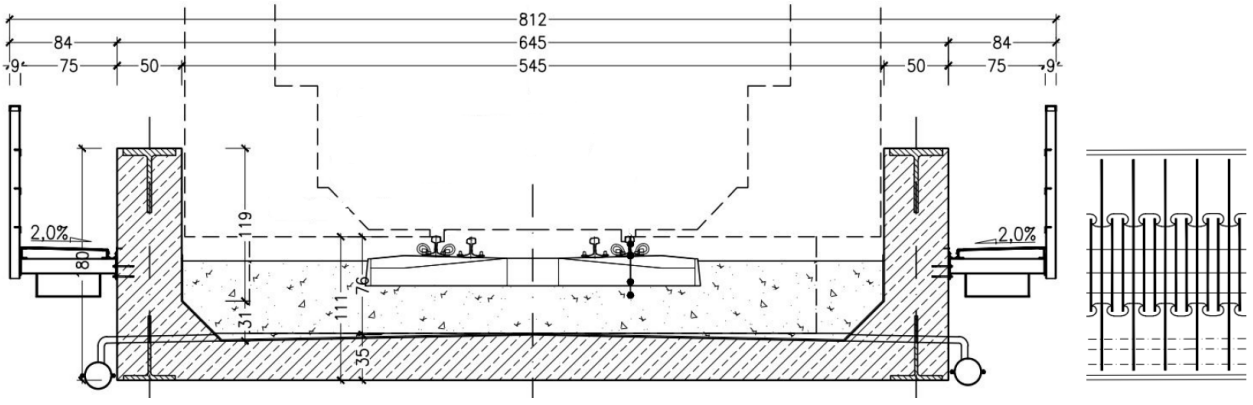

Figure 8: Cross section of the Dąbrowa Górnicza bridge and, on the right, longitudinal section showing the T-sections and rebar arrangement in the girder's web.

Figure 9: Bridge in Dąbrowa Górnicza after erection. Source: Nowak Mosty.

hybrid cross section is currently quite precise, the concept of a hybrid beam is not: in particular, it applies to a beam in which both hybrid and RC cross sections are used. In fact, the challenges encountered during the design of beams of the new bridge in Sobieszewo have shown that a new *hybrid beam concept* should be built. Also, just as the issue of shear force distribution is a key aspect of the *hybrid cross section concept*, the issue of the redistribution of bending moments due to concrete cracking and its rheology and proposing a general method for computer-aided modelling of hybrid beams are key aspects of a newly developing (and being the subject of the author's work) concept of a hybrid beam. As in the case of the hybrid section concept, in a hybrid beam concept also, the existing rules for global analysis of hybrid beams are not sufficient and a new concept should be built. In the Technical Specification of The European Committee for Standardization (CEN-TS approval) being created [11], the concept of a hybrid beam is directly related to the hybrid cross section used. In this article, the concept of a hybrid beam is considered more broadly: the use of a variable hybrid cross section may lead to a situation that in some places of the beam, the cross sections are *de facto* concrete (a very small share of structural steel). Practice confirms it [4]: a more general solution is used for the first bridges in the form of a beam in which the span sections are hybrid and the support sections are concrete. Such a type of beam is analysed in this article.

To sum up the problem of global analysis of hybrid beams, a comparison to both RC and steel–concrete composite beams is made briefly [9, 22]. In RC beams, if linear elastic analysis is assumed, it is allowed in ULS (Ultimate Limit State) to perform an uncracked analysis. Such an approach, presented in *Eurocode 2* [15], is justified because cracking of concrete in cross sections in both the span and support zones of continuous beams will not introduce significant changes in the distribution of the stiffness ratio of the span part to the support part along the length of the girder (compared to the original, uncracked state) (see Fig. 10a). The situation is quite different in the case of composite beams with a concrete slab on top of the steel I-section (e.g. in the cases described in *Eurocode 4* [17]). In the most common situation, a concrete slab in the mid-span will always be compressed as a result of the sagging bending moment. The situation is opposite in the support zones governed by a hogging bending moment. The concrete slab is there under tension and undergoes the cracking process, reducing the stiffness of the support sections, and thus, the stiffness distribution along the length of the girder changes. Cracking of concrete should be taken into account not only in dimensioning of cross sections (as in RC beams), but also in the linear elastic global analysis. General rules are given in *Eurocode 4* [17] for composite beams; for example, a cracked slab in the support zone can be assumed over a certain length, and additionally, in SLS (Serviceability Limit State), the increase of stresses in the reinforcement due to the effect of tension stiffening needs to be accounted for. Conducting a global analysis for hybrid beams goes beyond the rules included in available guidelines. Firstly, the cracking of the concrete slab itself cannot be modelled directly on the basis of simplified rules of *Eurocode 2* or *4*: if an uncracked slab is used in the analysis, the stiffness of the support zone is overestimated (very conservative and uneconomical for the reinforcement dimensioning) and the internal forces in the span part are underestimated; if accepting a slab as fully cracked, there are no guidelines on how to take into account the tension stiffening effect in SLS checks, for example, to check the crack width in the support zone. In such a case, support hogging moments would be underestimated in the global analysis. Secondly, the stiffness distribution along the length of the girders is also influenced by the cracking of the concrete web – both in the mid-span and in the support zones. Therefore, the following questions appear: how much of this web should be modelled as cracked and what stiffness of the cracked parts should be assumed? Moreover, these issues need to be analysed by also taking into account the change in the cross section from hybrid in mid-span to RC in the support zones – as in the bridge in Sobieszewo, or in currently designed bridges, for example, on the S3 road.

In addition, the application of general rules, for example, those defined in *Eurocode 4* [17], is very difficult because this standard was generally constructed assuming the use of beam models of class e^1 in the two-dimensional plane p^2 (introducing the nomenclature according to [23], where *e* stands for element type [dimension], *p* stands for

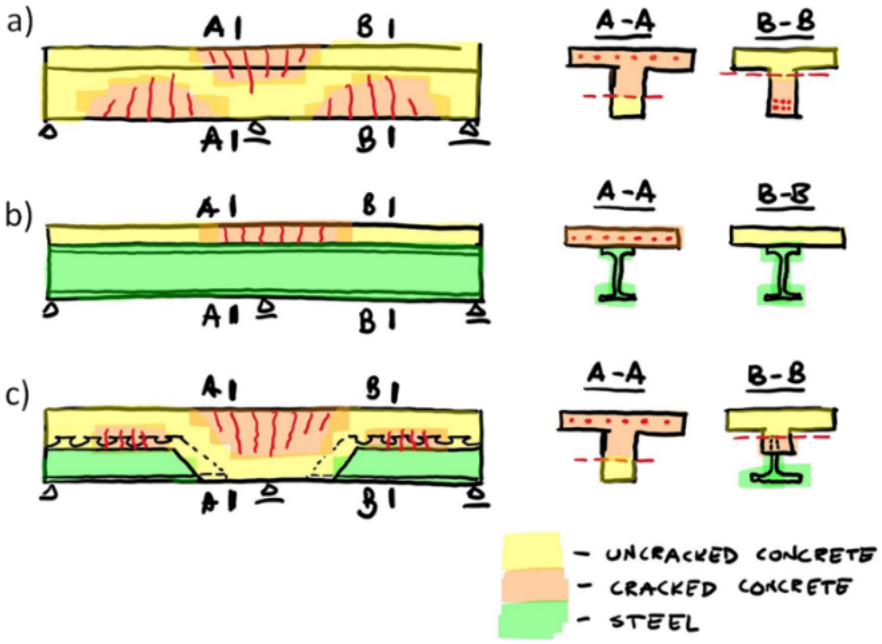

Figure 10: Concrete cracking ranges in (a) reinforced concrete beam, (b) composite beam, (c) hybrid beam.

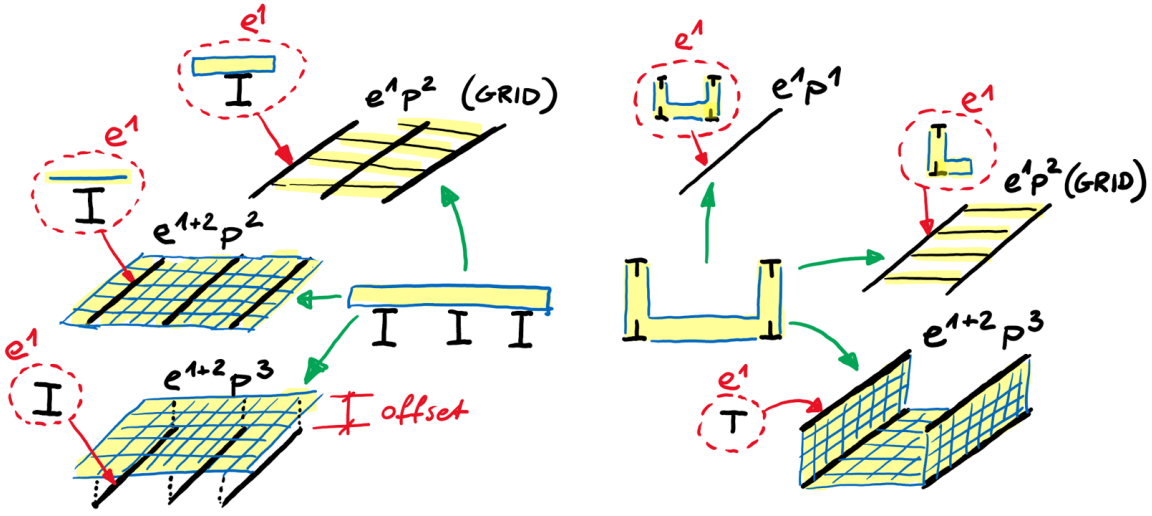

Figure 11: Different numerical models for composite bridges' analysis (on basis of [9]).

geometry of space [dimension] and 1, 2, 3 are numbers that describe it). In practice, more and more complex models (see Fig. 11) are often used when designing more and more complex construction forms. Simply, without 'complicating' computational models, it is no longer possible to reflect the complex behaviour of the structure considered. Apart from the e^1p^2 class grid models, it is currently a standard to use models of higher classes, for example, $e^{1+2}p^2$ models with the offset beam technique (deck slab modelled with shell elements, beams with bar elements) or models even more precise in which all elements are modelled with shell elements (e^2p^3). Such models allow for automatic accounting of shear lag effect (instead of the concept of the effective width of the concrete slab), but their main advantage over the grid models is the automatic transverse distribution of the loads between adjacent girders, as well as obtaining the actual internal forces in the concrete slab. Such models were used as an alternative to the grid models in the design of bridges described in Section 1.

The problem of using such models becomes evident when it is necessary to take into account concrete cracking. A typical example of such a situation is the arch or truss bridge with a deck in the level of tensile elements, but also an ordinary continuous beam, where the concrete slab is in tension in the zone of hogging moments, for example, in the bridge in Elbląg or Sobieszewo (Figs 2–6), or in both sagging and hogging moments, like in the bridge in Dąbrowa (Figs 8, 9). It is necessary to consider the stiffness decrease of shell elements in the main tension direction, which is caused by concrete cracking due to global effects. This problem also occurs when using grid models (e^1p^2), where it is important to properly reflect the introduction of forces into the tensile elements [24]. It is disputable not only how to determine the proper regions of cracked concrete and how to reduce its stiffness (considering the tension stiffening effect), but also how to apply it to the numerical model with shell elements. The introduction of reduced stiffness in the direction of global tension influences the stiffness in the other directions (the stiffness matrices of shell elements change) [25, 26]. In the grid model (or in an isolated beam), the reduction of the concrete stiffness related to its cracking influences only the bending stiffness EI of the considered beam, which is an elementary case. The opposite is the case when using shell elements. This is particularly noticeable in the e^2p^3 model (3d model with all elements modelled with shells), in which the concrete web is modelled with e^2 elements in the vertical plane (see, e.g. the bridge in Dąbrowa [13, 14]). If the stiffness in the longitudinal direction is significantly reduced, there is also a significant loss of the shear stiffness in the plane under consideration. The latter influences the shear flow between steel and concrete elements. There are currently no guidelines allowing for efficient (and accepted in engineering practice) modelling of considered types of structures (without considering complicated scientific models of concrete).

In this article, the influence of the following is discussed:

1. concrete cracking,
2. concrete rheology and
3. methods of computational modelling/determination of the range of the cracked zones

on the obtained values of internal forces in hybrid beams. Finally, a general *concept of* hybrid beams will be proposed, describing a proposal for efficient modelling of considered objects.

3 Finite Element (FE) analysis

In this section, numerical analysis will be carried out to show how the concrete cracked zones develop in a hybrid beam and how this phenomenon affects the bending moments' distribution along a beam. Influence of creep and shrinkage of concrete is also under investigation.

3.1 Numerical models

As an example for numerical investigation, exemplary girder from a newly designed bridge on S3 road was adopted. Geometry of this girder is shown in Fig. 12. For the purpose of analysis, it is assumed that *in situ* concrete slab (concrete C30/37), with a thickness of 24 cm, is casted with fully propped precast girder (which is made out of S460N steel and C50/60 concrete). Thus, after removing the temporary supports, it is subjected to participate in the actions taken from its self-weight too. Longitudinal reinforcement in hogging moments zone is in

- *in situ* slab: arranged in two layers, upper #25/100, lower #20/100;
- upper slab of precast element: arranged in one layer, #20/150 and
- web of precast element: both sided #10/100.

Reinforcing steel in compressed concrete is omitted in the analysis in approaches A and B. In approach C, reinforcement is considered in every stress state, no matter whether it is compressed or tensioned. The hybrid beam is thus modelled as a structure consisting of five materials: one steel and four types of homogenised RC (*in situ* slab, upper slab of precast element, web of precast element, bottom slab of precast element – all of these with different concrete class and/or reinforcement ratio). Appropriate stress–strain curves are assigned for the entire regions with the same concrete thickness, concrete class and reinforcement ratio. Geometry of the beam is presented in Fig. 12.

Actions applied to the girder were taken directly from a real bridge analysis as

- self-weight of the precast element + *in situ* slab (density of concrete 25 kN/m^3, of steel 78.5 kN/m^3);
- self-weight of surface layers – as uniformly distributed with a value of 2.65 kPa;
- uniformly distributed load (UDL) – 9 kPa, applied to the first, second or both spans and
- tandem system (TS) load – 2x 300 kN moving along the entire girder.

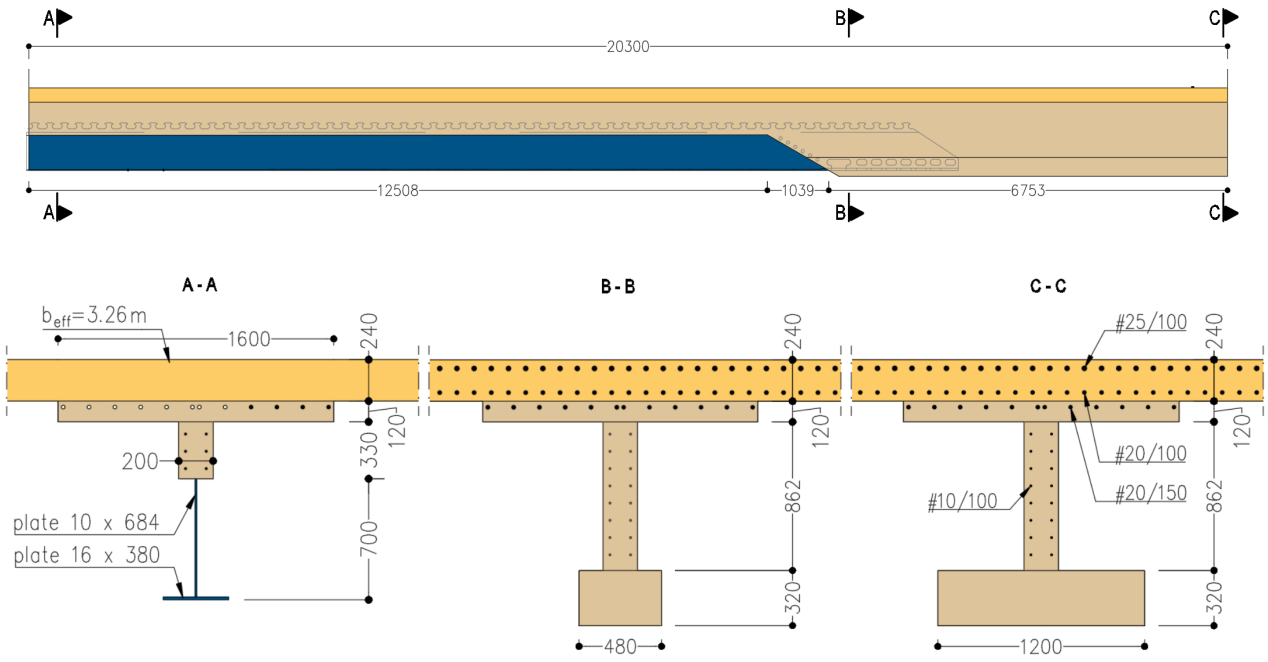

Figure 12: Hybrid beam assumed for FE analysis (rebars only in the tensile regions are displayed).

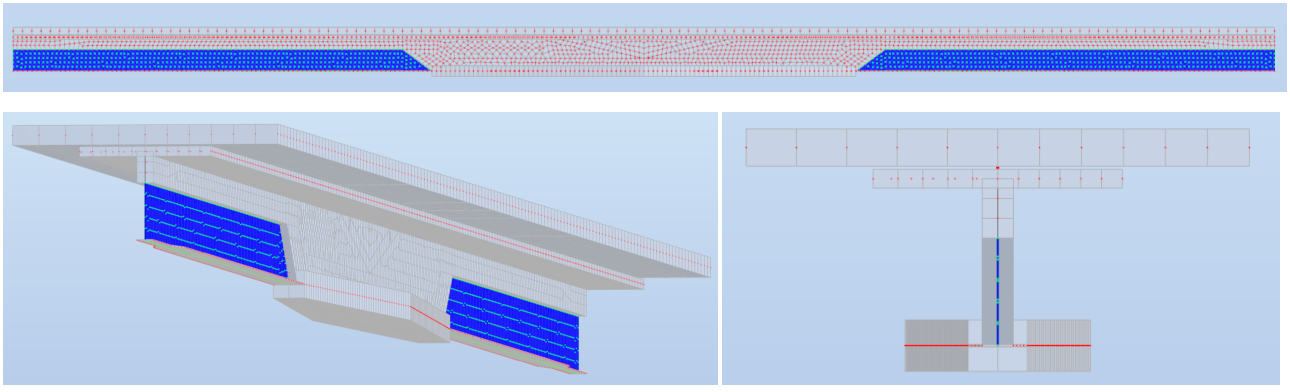

Figure 13: Side view, 3d view and cross section of a finite element model of the considered beam (steel web highlighted in blue).

These loads allowed to obtain bending moments in a girder that are very close to moments in a real bridge, thus real cracking conditions are expected. The FE model was made in e^2p^3 class with all elements modelized with shell elements, as shown in Fig. 13.

3.2 Cracking of concrete

To investigate the influence of concrete cracking on the bending moment distribution along a beam length, three different approaches were adopted. They are as follows:

– Approach A: iterative procedure. First, the stress envelope for characteristic combinations is calculated using the uncracked sections' stiffness (uncracked analysis). In regions where the tensile stress in the concrete exceeds twice the strength f_{ctm} due to the envelope of global effects, the stiffness is reduced to cracked sections' stiffness and calculations are repeated. Again, the stress layout is checked in all elements, and in regions where the tensile stress in the concrete exceeds twice the strength f_{ctm} due to the envelope of global effects, the stiffness is reduced to cracked sections' stiffness. This procedure is repeated iteratively until there are no regions with tensile stress

more than $2f_{ctm}$ (where f_{ctm} = 2.90 MPa and 4.07 MPa for concrete C30/37 and C50/60, respectively). This approach is based on a similar approach adopted in *Eurocode 4* [17], but it is extended to the iterative procedure (reasons will be explained hereafter).

– Approach B: simplified method. It is based again on the analogy to *Eurocode 4* [17] regulations with some modifications. It is assumed that 15% of the span length on each side of each internal support is under significant hogging bending moment and approx. 60% of a side span is under significant sagging bending moment. Thus, tensile concrete in these regions will undergo cracking process. As a simplification, tensile concrete is assumed to be cracked if the tensile stress is greater than 0. This way, no iterative procedure is needed because the borders between the cracked and uncracked sections are defined only with geometric parameters (length of spans and neutral axis of sections).
– Approach C: automatic non-linear analysis based on pre-defined concrete material laws, considering the changes in concrete stiffness depending on the principal stress in finite elements.

In approaches A and B for uncracked sections, material stiffness was calculated automatically on the basis of Young modulus (E_{cm} = 32.8 and 37.3 GPa for C30/37 and C50/60, respectively) and Poisson's coefficient ν = 0.20. For cracked concrete sections, the modification of stiffness matrix was made this way to obtain, for longitudinal direction, reduced stiffness standing only for the stiffness of reinforcement, but taking into account tension stiffness effect according to [27] annex L1 and [17, 24, 28]. This way, the tension member stiffness was defined as

$$(E_s A_s)_{\text{eff}} = \frac{E_s A_s}{1 - 0.35/(1 + n_0 \rho_s)}$$

$E_s A_s$ stands for modulus of elasticity and area of reinforcement, n_0 for E_a/E_{cm} ratio and ρ_s for the area of rebar to concrete ratio (A_s/A_c). The Poisson coefficient was adopted to be 0. For transversal and diagonal directions, the stiffness was defined like for uncracked sections, not to influence the shearing stiffness in a plane of shell elements.

For approach C, the following law for concrete elements was adopted (with distinction to elements with different reinforcement layouts). RC parts were modelled using a homogenised material that enabled considering tension stiffening effect for reinforcement and tension softening of the concrete by applying one stress–strain curve for each part of the RC members. This model is based on the stress–strain and force–strain relationships presented in [27-29]. These relationships were originally defined for embedded reinforcing steel, but the authors adopted them to concrete parts.

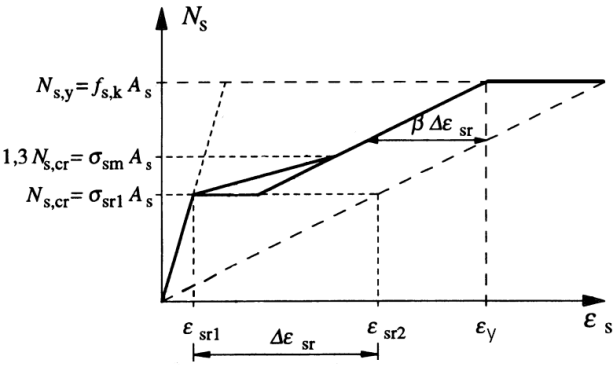

Figure 14: Tension stiffening model adopted in approach C according to annex L1 [27].

This approach of modelling of cracked reinforced parts is not strict and has some apparent inconsistencies. Firstly, longitudinal reinforcement may not be oriented in the same direction as principial stresses in the concrete. Tension stiffening effect is calculated on the basis of longitudinal reinfocement, but appears in finite element model in the direction of principal stresses. Moreover, when crack appears, Poisson's coefficient in the concrete could be reduced to 0 value, which also would affect the stiffness matrix in a two-dimensional shell finite element. Despite the abovementioned doubts presented in Fig. 14, the model law for concrete materials was adopted in approach C analysis as a sufficient and relatively easy method in implementation of engineering approximation.

The models in approaches A–C are different also due to fact that they induce concrete cracking at different tensile stress levels: $2f_{ctm}$ in approach A, 0 but at *ad hoc*-prescribed regions of the beam in approach B and f_{ctm} in approach C.

3.3 Concrete rheology

Similar approaches were considered for estimation of concrete creeping and shrinkage in a hybrid beam. Results presented hereafter were obtained with the following assumptions:

1. For approaches A and B, creep coefficients 2.13 and 1.52 were taken for C30/37 and C50/60 elements, respectively, and shrinkage strain was assumed to be

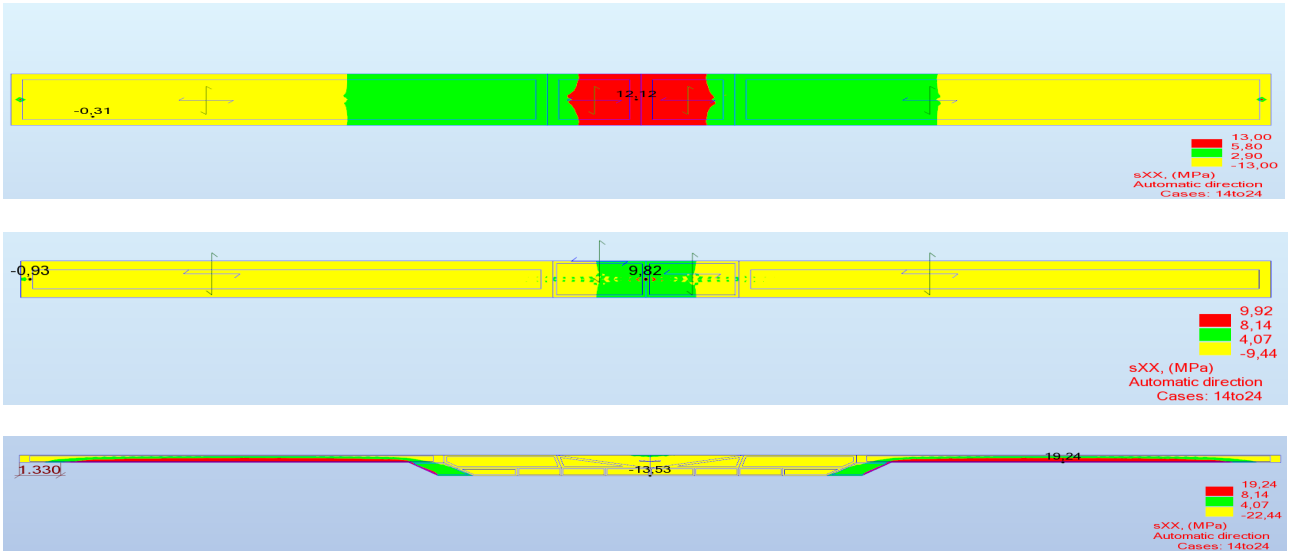

Figure 15: Tensile stress layout in *in situ* slab (top view), upper slab (top view) and concrete web of the prefab (side view) – uncracked analysis (step 1).

0.34‰ and 0.36‰, respectively. Creep coefficients were taken to reduce the E_{cm} of uncracked concrete elements (as a simplification using the analogy to commonly used regulation of EC4 [17]).

2. For approach C, a rheology of concrete was considered by the so-called strain approach, default for CSM (Construction Stage Manager) in SOFiSTiK software [30].
3. Shrinkage strains were applied only to uncracked concrete, which is an analogy to [17] regulation which states that '*in regions where the concrete slab is assumed to be cracked, the primary effects due to shrinkage may be neglected in the calculation of secondary effects*'.

3.4 Results

First, the results of analysis with approach A are presented. In the following figures, it is presented how the tensile zones in concrete develop. Maps of tensile stress are presented in an upper *in situ* slab, an upper prefab slab and a prefab web. Red-coloured regions denote tensile stress bigger than $2f_{ctm}$, green-coloured regions indicate tensile stress in the range of f_{ctm}–$2f_{ctm}$, and in yellow-marked regions, the tension does not exceed f_{ctm}. For the uncracked analysis (Fig. 15), it is observed that stresses exceeding $2f_{ctm}$ are present only in the *in situ* slab at about 11% of the span length in each side of the internal support and partly in the concrete web in the mid-span region. Upper prefab slab and prefab web in the support zone resist smaller tensile stress, so they can be assumed to be uncracked in the next step.

After reducing the stiffness in red highlighted regions, calculations were redone and new stress layouts were analysed (Fig. 16). As expected, a new analysis caused reduction of tensile stress in the *in situ* slab and a very significant increase of tensile stress in the prefab, both upper slab and web. Tensile stress exceeds $2f_{ctm}$ in this region, so they will undergo cracking (reduction of their stiffness).

Repeated calculations with decreased stiffness of newly cracked elements showed decrease of tensile stress in the prefab upper slab, noticeable increase of tension in the *in situ* slab and very significant increase of tensile stress in the prefab web (see Fig. 17). This way, a cracked zone in the prefab web develops.

Multiple updates of cracked zone range and recalculations cause a minor increase of the cracked zone in the web close to the internal support, and finally, the stable state can be found (let it be named step 4; despite that, in fact, seven iterations were needed to get the final state of cracking in case of considered beam). Changes in stress layout are hardly visible compared to this in Fig. 17, so no further maps of tensile stress are presented. Approach A makes it possible to observe a continuous development of the cracked zones until their final state. In approach B, the cracked zones are *ad hoc* prescribed to the structure. In approach C, the cracked zones are determined automatically in non-linear calculations and are different in every considered combination of actions (which is also doubtful because once cracked, concrete should remain

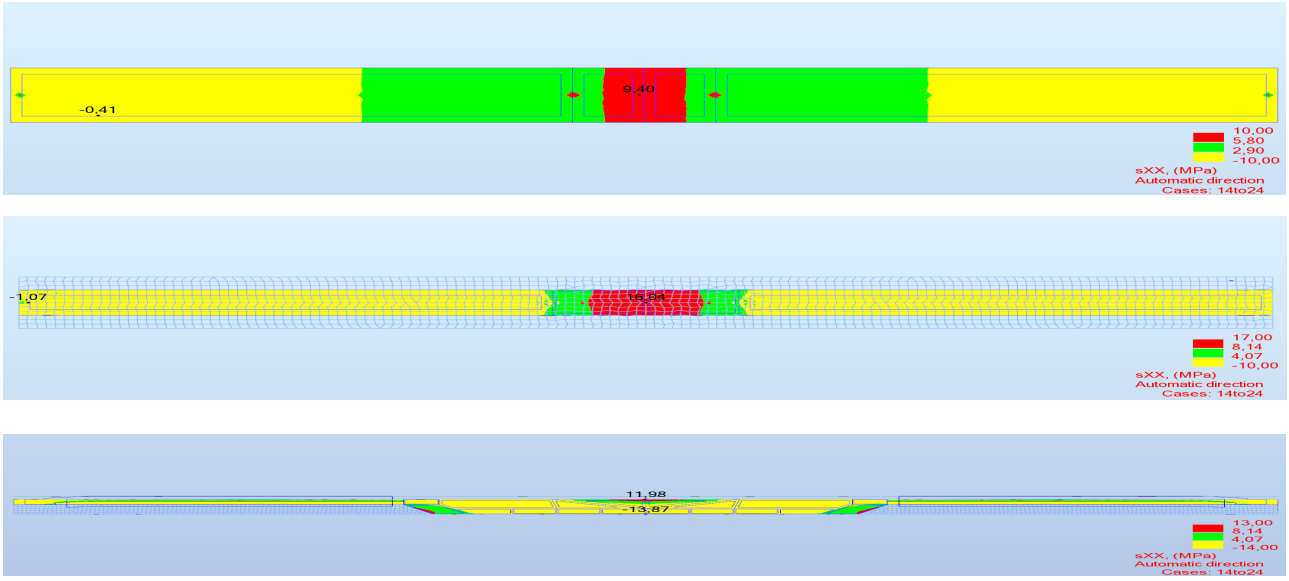

Figure 16: Tensile stress layout in *in situ* slab (top view), upper slab (top view) and concrete web of the prefab (side view) – cracked analysis (step 2).

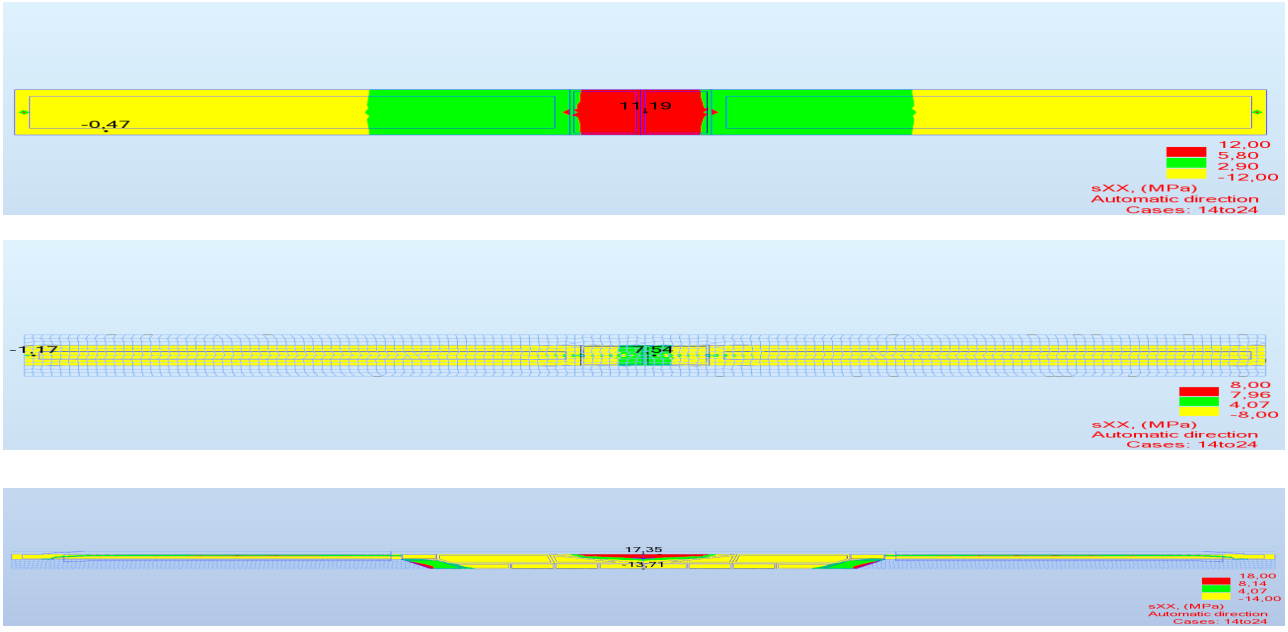

Figure 17: Tensile stress layout in *in situ* slab (top view), upper slab (top view) and concrete web of the prefab (side view) – cracked analysis (step 3).

with decreased stiffness also for other combinations). Differences in cracked regions in approaches A, B and C are shown in Fig. 18.

Changes in bending moment envelope depend on the assumed approach and the cracking zone development in approach A, which are presented in Fig. 19 and Table 1. In Table 1, relative changes in extreme sagging and hogging bending moments in relation to results from uncracked analysis are presented.

Similar simulation is made to show how the concrete creeping influences bending moment distribution along the beam (Fig. 20 and Table 2).

Fig. 21 and Tab. 3 shows secondary bending moments due to shrinkage.

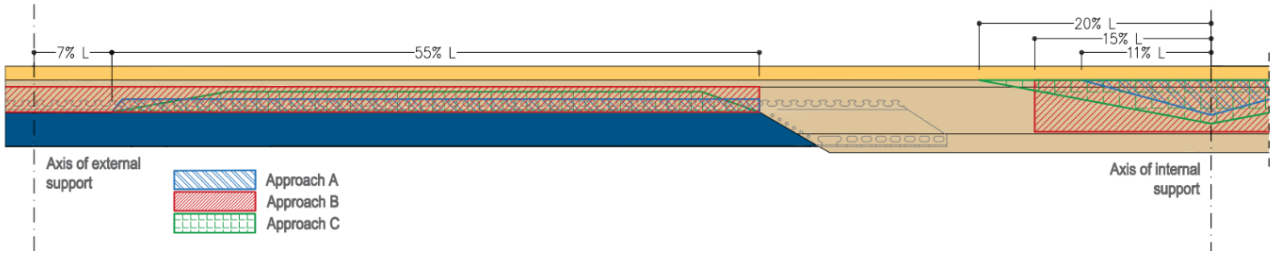

Figure 18: Comparison of cracked zones in the web in approaches A, B and C. Cracked zones in slabs are equal to the length of cracked zones in the top part of a web at the internal support.

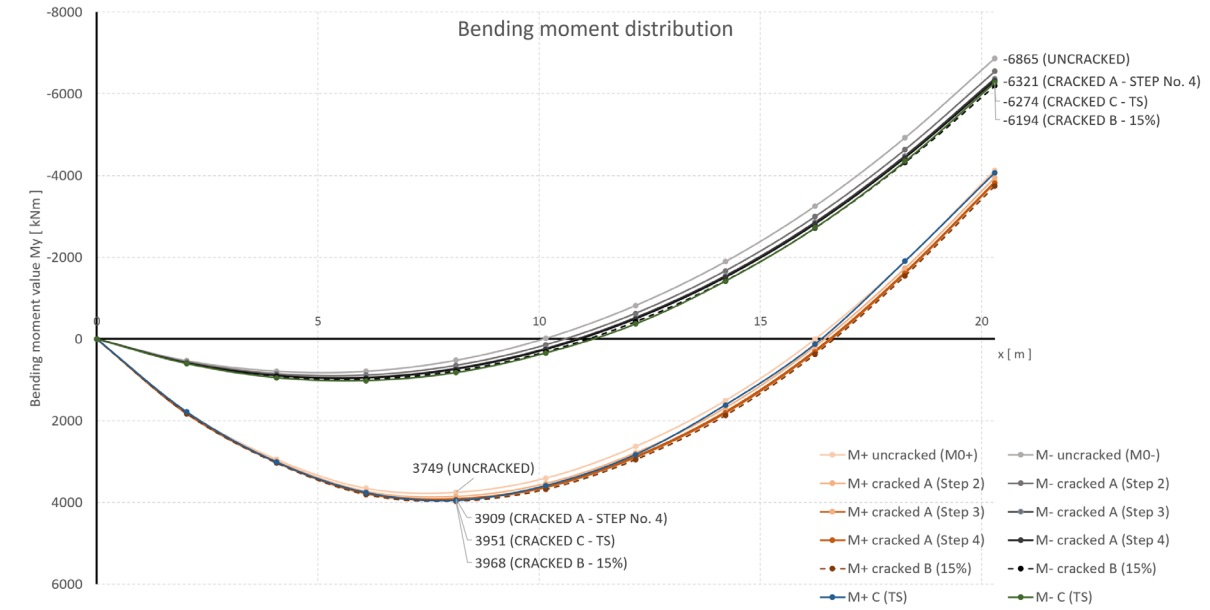

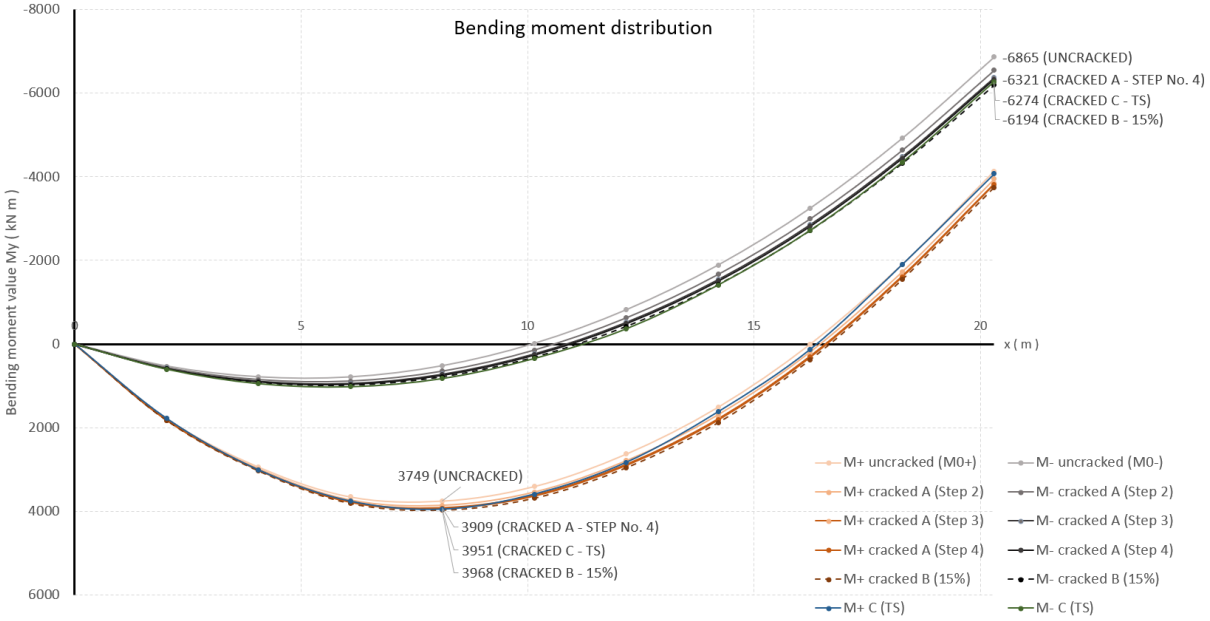

Figure 19: Bending moment envelope depending on the assumed approach (A, B, C).

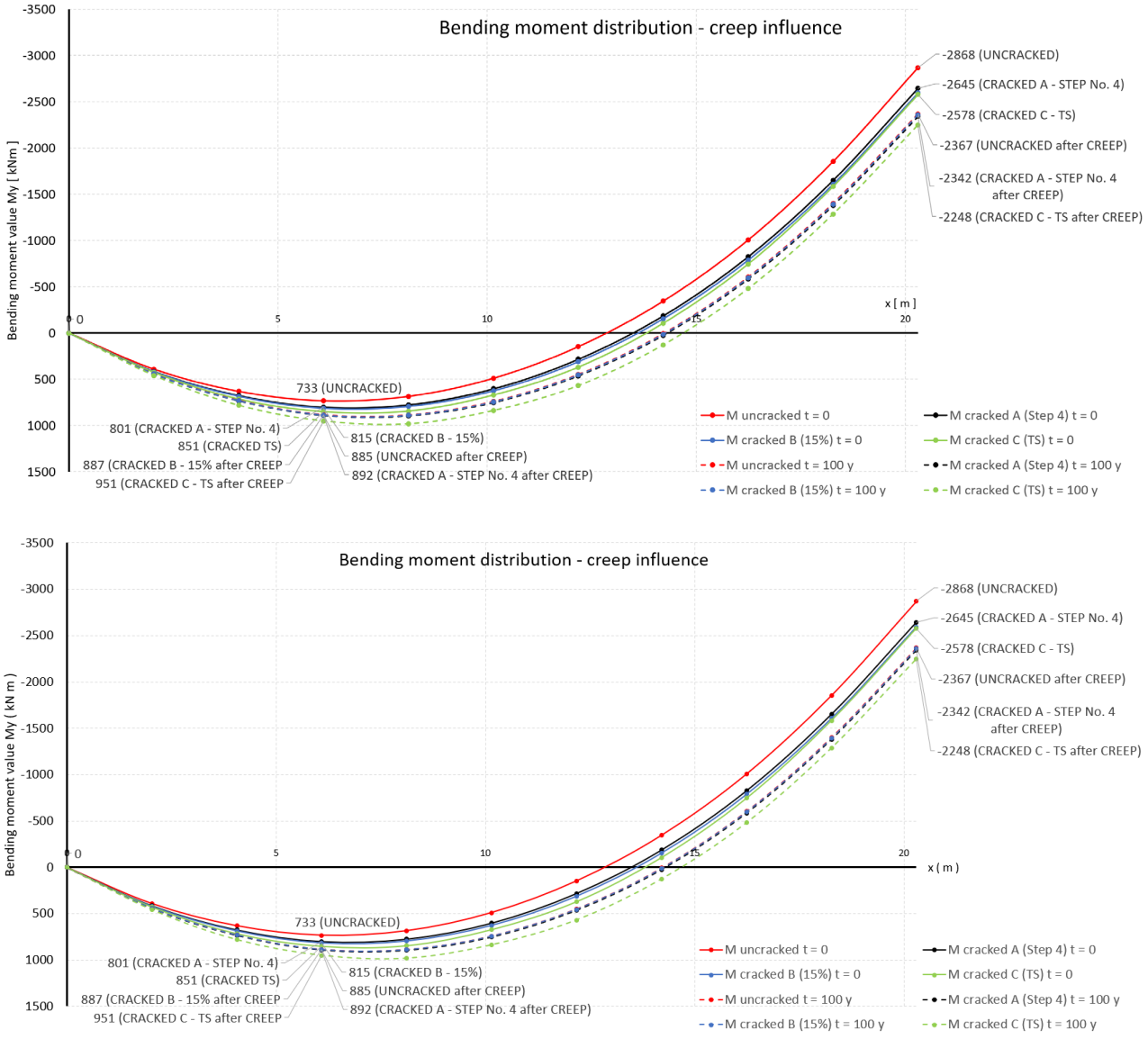

Figure 20: Influence of creep on the bending moment distribution in dependence of the assumed approach (A, B, C). Continuous lines – bending moments without creep, dotted lines – after creeping of concrete.

4 Discussion

1. Cracking of concrete influences the bending moment distribution along a beam. In fact, the range of cracked zones due to external loads is much bigger in support zone sections that are entirely made out of concrete than in mid-span sections that are predominantly made out of structural steel in a tensile zone. This means that the reduction of beam's inertia at the internal support is bigger than that in the mid-span and, due to cracking, the hogging moments decrease (about 8%–10%) and the sagging ones increase (about 5%–6%) in comparison to uncracked analysis.
2. Irrespective of the assumed approach (A, B or C), the obtained results are in a good convergence. Differences in final bending moments envelopes do not exceed 2%. This means that, if cracking is considered, the cracked range itself has a minor impact on the results of analysis.
3. Creep of concrete causes further redistribution of bending moments. Approaches A and B give nearly the same results, while in approach C, the obtained results differ slightly (bigger shift of the entire bending moment diagram towards the sagging moments). This can be explained by the fact that in a combination of self-weight loads, a model including automatic

Table 1: Bending moment values (kN m) along the girder's length (m), depending on the assumed approach (A, B, C). Numerical interpretation of Fig. 19.

	No.	0	1	2	3	4	5	6	7	8	9	10	M+ / M0+	M- / M0-
Approach	x [m]	0	2,03	4,06	6,09	8,12	10,15	12,18	14,21	16,24	18,27	20,3		
Base state	M+ uncracked (M0+)	0	1782	2940	3652	3749	3401	2626	1505	1	-1902	-4129	100,0%	
	M- uncracked (M0-)	0	529	787	789	520	-16	-820	-1892	-3252	-4922	-6865		100,0%
A	M+ cracked A (Step 2)	0	1804	2984	3727	3853	3535	2786	1684	183	-1730	-3947	102,8%	
	M- cracked A (Step 2)	0	561	850	885	648	143	-628	-1668	-2996	-4634	-6547		95,4%
	M+ cracked A (Step 3)	0	1816	3009	3768	3909	3607	2870	1779	279	-1637	-3845	104,3%	
	M- cracked A (Step 3)	0	579	884	936	716	229	-526	-1548	-2860	-4481	-6369		92,8%
	M+ cracked A (Step 4)	0	1820	3017	3782	3928	3630	2898	1811	312	-1607	-3819	104,8%	
	M- cracked A (Step 4)	0	584	896	953	739	257	-492	-1508	-2814	-4432	-6321		92,1%
B	M+ cracked B (15%)	0	1829	3035	3811	3968	3682	2954	1873	372	-1544	-3748	105,8%	
	M- cracked B (15%)	0	597	920	990	787	318	-419	-1423	-2717	-4321	-6194		90,2%
C	M+ C (TS)	0	1781	3012	3760	3951	3590	2828	1616	125	-1902	-4068	105,4%	
	M- C (TS)	0	602	947	1019	824	343	-366	-1415	-2719	-4346	-6274		91,4%

Table 2: Bending moment values (kN m) along the girder's length (m0 due to creep in dependence of the assumed approach (A, B, C). Numerical interpretation of Fig. 20.

	No.	0	1	2	3	4	5	6	7	8	9	10	M+ / M0+	M- / M0-
Approach	x [m]	0	2,03	4,06	6,09	8,12	10,15	12,18	14,21	16,24	18,27	20,3		
Base state	M uncracked t = 0	0	391	631	733	685	489	147	-345	-1006	-1853	-2868	100,0%	100,0%
	M uncracked t = 100 y	0	442	730	885	887	741	449	8	-603	-1401	-2367	120,7%	82,5%
A	M cracked A (Step 4) t = 100 y	0	442	731	886	888	844	452	12	-599	-1397	-2364	109,3%	92,2%
	M cracked A (Step 4) t = 100 y	0	444	735	892	896	753	464	25	-584	-1379	-2342	121,7%	81,7%
B	M cracked B (15%) t = 0	0	419	685	815	794	626	311	-154	-788	-1607	-2595	111,2%	90,5%
	M cracked B (15%) t = 100 y	0	442	731	887	889	744	453	13	-598	-1393	-2360	121,0%	82,3%
C	M cracked C (TS) t = 0	0	0	427	715	851	845	672	370	-105	-746	-1584	116,1%	89,9%
	M cracked C (TS) t = 100 y	0	0	459	782	951	982	838	569	128	-480	-1286	129,7%	78,4%

reduction of stiffness due to cracking (approach C) has a greater crack range (cracking occurs at f_{ctm} stress) that the models in approaches A and B (cracking occurs at $2f_{ctm}$). This can be clearly observed in Table 2 approach C: even without consideration of creep (t = 0), the bending moment diagram is shifted towards sagging moments (compared to approaches A and B). The change due to creep itself is similar for all approaches (A, B, C). For uncracked analysis creep influence is slightly bigger (comparing to approaches A, B, C), what can be explained by the fact that creep strains increase also in tensile uncracked concrete sections' parts (mainly close to the internal support).

4. Final bending moments after creep of concrete are very similar for both cracked and uncracked analyses. The convergence of these results obviously depends on the reinforcement ratio and creep coefficient, but it can be generally concluded that for some limits of the latter, the cracking itself will not influence significantly moments' redistribution due to creeping.
5. For the considered beam, the actual decrease in hogging bending moment due to creep varies (depending on the approach A–C for cracked analysis) from 230 to 330 kN m, while hogging moment from external loads is of about 6300 kN m. For uncracked analysis the decrease of bending moments due to

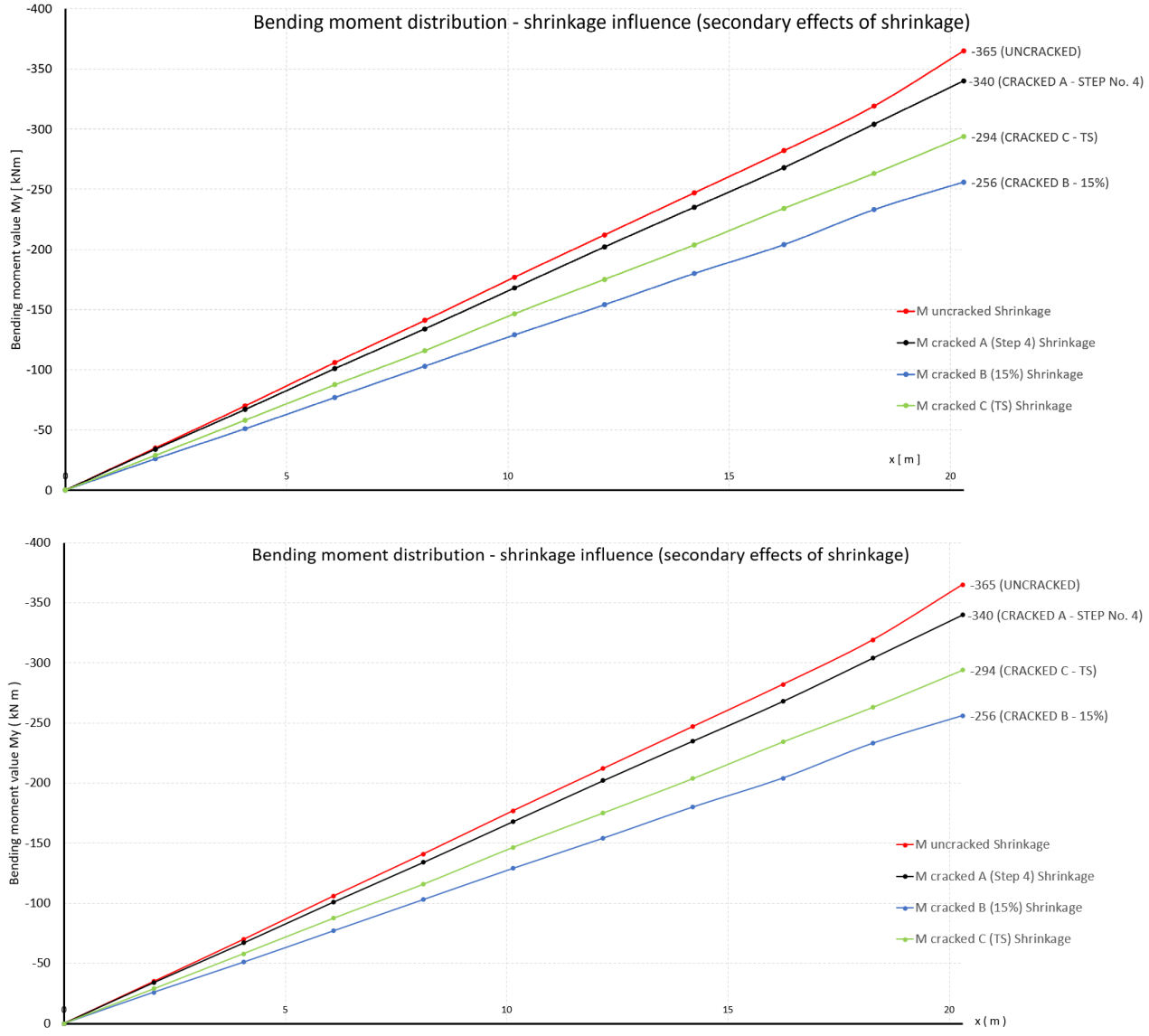

Figure 21: Bending moment distribution due to shrinkage in dependence of the assumed approach (A, B, C).

creep is about 500 kN m comparing to 6870 kN m of the total hogging moment. Thus, the change is up to approx. 4%–5% for cracked analysis and about 7% for uncracked one. Similarly, increase in sagging moment of 100–140 kN m in relation to moment from external loads of about 3900 kN m gives a change of about 3.5% for cracked analysis and, by analogy, about 200 / 3750 = 5.5% for uncracked one.

6. Secondary moments caused by concrete shrinkage depend on the cracked zone ranges along the beam length. Because shrinkage strains were applied to the structure's parts that are not cracked, direct comparison of secondary moments cannot be made (different assumptions for every model). For approach C, the direction of concrete softening due to cracking is different, as it depends on the principal stress direction. But it can be noticed that despite the fact that there are significant percentage differences between particular approaches, the actual results are quite similar. Relative differences in bending moments up to 30% (between uncracked analysis and approach B) turn out to be of minor importance, considering the real differences of up to 110 kN m (for the considered beam), which is about 2% of the hogging moments induced by the external loads (about 6300 kN m for cracked analysis). The overall share of secondary shrinkage moments in entire bending moments is about 4%–5%.

Table 3: Bending moment values (kN m) along the girder's length (m) due to shrinkage in dependence of the assumed approach (A, B, C). Numerical interpretation of Fig. 21.

Approach	No.	0	1	2	3	4	5	6	7	8	9	10	M- / M0-
	x [m]	0	2,03	4,06	6,09	8,12	10,15	12,18	14,21	16,24	18,27	20,3	
Base state	M uncracked Shrinkage	0	-35	-70	-106	-141	-177	-212	-247	-282	-319	-365	100,0%
A	M cracked A (Step 4) Shrinkage	0	-34	-67	-101	-134	-168	-202	-235	-268	-304	-340	93,2%
B	M cracked B (15%) Shrinkage	0	-26	-51	-77	-103	-129	-154	-180	-204	-233	-256	70,1%
C	M cracked C (TS) Shrinkage	0	-29	-58	-88	-116	-147	-175	-204	-234	-263	-294	80,5%

5 Conclusions and design concept of the hybrid beam

Analysis of the obtained results confirms that both cracking of concrete and rheology of concrete influence bending moment distribution along the beam. Cracking of concrete induces the most significant changes, while changes due to creep and shrinkage affect the bending moment less severely. Moreover, creep shifts the bending moment diagram towards sagging moments, while shrinkage shifts it towards hogging ones, reducing the influence of the previous one. Considering that creep affects the bending moment values of 4%–7% and shrinkage of 4%–5% (in opposite directions), one can state that the rheology of concrete is of minor importance in a design of hybrid beams. In classic composite beams, in which concrete slab is placed on the top of steel I-beam, after cracking of concrete in the internal support zones, the rheology of concrete is induced only in mid-span sections (where concrete is under compression). Support sections (I-beam + rebar in the slab) restrain deformation due to concrete rheology, and significant secondary moments appear. On the contrary, in hybrid beams, uncracked concrete parts are both in mid-span and support zones, and due to concrete rheology, the entire beam undergoes deformations with limited internal restraint. Secondary moments due to creep and shrinkage are thus limited to less significant values.

Regions where concrete should be assumed to be cracked cannot be directly established according to the procedure presented in [17]. It means it is not enough to perform at first uncracked analysis, then to reduce axial stiffness for places where the tensile stress exceeds $2f_{ctm}$ and then to recalculate a static system. It has been proven in Section 3.4 that such an approach should be iterative, as changes in stiffness of one part influence the tensile force redistribution in the entire element, including the web of a beam. Such an approach seems to be impractical for engineering application. Similarly, approaches based on non-linear analysis (like the presented approach C) seem to be too complicated for a design based on many combination of actions, simply too much of computational power would be required. Another problem is proper determination of stiffness matrix for shell elements undergoing cracking process in a certain direction. This is problematic to ensure a proper axial stiffness and, at the same time, proper stiffness for in-plane shearing of planar finite elements.

Taking the abovementioned into account, it seems to be reasonable to accept the design concept in which for global elastic analysis, the entire structure would be *modelled with uncracked sections*. Bending moments obtained this way could be further modified by their multiplication by appropriate coefficients, which could reduce hogging and increase sagging bending moments. Such an approach is not a novum and is already widely accepted for classic composite beams, for example, in p. 5.4.4 [17], if certain conditions are fulfilled, limited redistribution in the per cent of initial hogging moments is allowed. On the basis of presented studies of one particular hybrid beam authors could proposeto perform uncracked analysis and:

- for dimensioning of internal support sections: to limit a redistribution of hogging moments to, for example, 5% (which is on the safe side because real decrease of hogging moment comparing to the one obtained from uncracked analysis is about 8%–10% due to cracking, 4%–7% due to creeping and –4%–5% due to shrinkage, and overall, it is up to 5%–10%, so more than the assumed 5%);
- for dimensioning of mid-span sections: to limit a redistribution of hogging moments to, for example, 15% (which is on the safe side because real decrease of hogging moment comparing to the one obtained from uncracked analysis is about 8%–10% due to cracking, 4%–7% due to creeping and –4%–5% due to shrinkage, and overall, it is up to 5%–10%, so less than the assumed 15%).

Determination of exact limits of redistribution should be based on the analysis of many different hybrid beams and, therefore, parametric studies. Such studies are currently the subject of the author's work.

Thus, in this article, the authors actually propose a complete reversal of the concept used as standard in EC4 for the needs of the hybrid beam: uncracked analysis. The presented concept of global elastic analysis enables easy modelling of hybrid beams with safe-sided assumptions for both hogging and sagging moment regions. The above is the result of a broader look at the experience in the design and construction of structures presented in [4], and the beam analysis presented in this paper is an example that enables a quantitative assessment of the problem.

References

[1] Seidl G., Viefhues E., Berthellemy J., Mangerig I., Wagner R., Lorenc W., Kożuch M., Franssen J.M., Janssen D., Ikäheimonen J., Lundmark R., Hechler O., Popa N., RFCS research project *PrEco-Beam: Prefabricated enduring composite beams based on innovative shear transmission*. EUR 25321 EN. Brussels, European Commission, 2013.

[2] Feldmann M., Möller F., Möller S., Collin P., Hällmark R., Kerokoski O., Lorenc W., Kożuch M., Rowiński S., Nilsson M., Astrom L., Norlin B., Seidl G., Hehne T., Hoyer O., Stambuk M., Hariu T., *ELEM: Composite bridges with prefabricated decks*. EUR 25897 EN. Brussels, European Commission, 2013.

[3] Seidl G., Popa N., Zanon R., Lorenc W., Kożuch M., Rowiński S., Franssen J.-M., Fohn T., Hermosilla C., Farhang A., Nüsse G. RFCS dissemination knowledge project *PRECO+: Prefabricated Enduring Composite Beams based on Innovative Shear Transmission*. EUR 27834 EN, Brussels, European Commission, 2014.

[4] Lorenc W., *Composite dowels: the way to the new forms of steel-concrete composite structures*, IABSE Symposium: Synergy of Culture and Civil Engineering – History and Challenges, 7-9 October 2020, Wrocław, Poland.

[5] Lorenc W., Kołakowski T., Hukowicz A., Seidl G., *Verbundbrücke bei Elbląg Weiterentwicklung der VFT-WIB-Bauweise*, Stahlbau 86, Heft 2, 2017.

[6] Lorenc W., Seidl G., *Innovative Konstruktionen im Verbundbrückenbau mit Verbunddübelleisten*, Stahlbau 87, Heft 6, 2018.

[7] Kozioł P., *Nośność łączników stalowych w strefie połączenia elementu zespolonego z elementem betonowym*, Raport serii PRE nr 3/2018. Praca doktorska. Politechnika Wrocławska, 2018 (PhD dissertation – in Polish).

[8] Kozioł P., Kożuch M., Lorenc W., Rowiński S., *Connection capacity of the transition zone in steel-concrete hybrid beam*, Civil and Environmental Engineering Reports, CEER 2017; 25(2), p. 137-146.

[9] Lorenc W., Kożuch M., *Introduction to hybrid sections and hybrid beams in bridges*, WDM Symposium 2021, Wrocław, Poland.

[10] Allgemeine bauaufsichtliche Zulassung Z-26.4-56 *Verbunddübelleisten*, Deutsches Institüt für Bautechnik.

[11] CEN TS *Composite Dowels*, Draft.

[12] Feldmann M., Kopp M., Pak D., *Composite dowels as shear connectors for composite beams – background to the German technical approval*, Steel Construction 9 (2016), No. 2, p. 80-88.

[13] Bartoszek B., Stempniewicz A., Ochojski W., Adamczyk A., Natonek G., Lorenc W., *Railway bridge in Dąbrowa Górnicza using composite dowels: new system development of composite railway bridges (Most kolejowy w Dąbrowie Górniczej z zastosowaniem zespolenia composite dowels: opracowanie nowego system zespolonych mostów kolejowych)*, WDM Symposium 2019, Wrocław, Poland.

[14] Lorenc W., Stempniewicz A., Bartoszek B., *New kind of externally reinforced structure of railway bridge with low construction height using rolled sections and composite dowels*, ArcelorMittal.

[15] EN 1992, *Eurocode 2: Design of concrete structures* (all parts).

[16] EN 1993, *Eurocode 3: Design of steel structures* (all parts).

[17] EN 1994, *Eurocode 4: Design of composite steel and concrete structures* (all parts).

[18] Johnson R., *Vertical shear in hybrid composite cross-sections of beams*, WDM Symposium 2021, Wrocław, Poland.

[19] Lorenc W., *Przenoszenie siły poprzecznej a definicja konstrukcji zespolonej*. Mosty 2011/6.

[20] Lorenc W., *The model for a general composite section resulting from the introduction of composite dowels*, Steel Construction, 10, No. 2, p. 154-167.

[21] Lorenc W., Balcerowiak S., Czajkowski J., Dobrzański J., *The coherent concept of the lever arm in a cross-section*, IABSE Symposium 2020, Wrocław, Poland.

[22] Kożuch M., *Belki hybrydowe w mostach: definicja i koncepcja projektowania*, Mosty 4/21 p. 40-42.

[23] Bień J., *Modelling of structure geometry in Bridge Management Systems*, Archives of Civil and Mechanical Engineering, Vol. XI, No. 3, 2011, s. 519-532.

[24] Johnson R., *Analyses of a composite bowstring truss with tension stiffening*, Proceedings of the Institution of Civil Engineers, Bridge Engineering I56, Issue BE2, 2003, p. 63-70.

[25] Aditya S., Sri T., Ay Lie H., *Modelling the relationship of the flexural rigidity factor and reinforcement ratio by numerical simulation*, Procedia Engineering 95 (2014), p. 241-251.

[26] Ugural A., Plates and shells. Theory and Analysis., CRC Press, Taylor & Francis Group 2018.

[27] ENV 1994-2: 2001, *Eurocode 4: Design of composite steel and concrete structures, Part 2: composite bridges*.

[28] Hendry C., Johnson P., *Designers' guide to EN 1994-2 Eurocode 4: Design of steel and composite structures*, Thomas Telford, 2006.

[29] CEP-FIB Model Code 1990, Thomas Telford, 1993.

[30] SOFiSTiK 2020: ASE (General Static Analysis of Finite Element Structures) Manual, Oberschleißheim, Germany, 2020.